Photocatalytic Activity of TiO2 Nanoparticles Sensitized by CuInS2 Quantum Dots

ARTICLE *in* INDUSTRIAL & ENGINEERING CHEMISTRY RESEARCH · JULY 2011

Impact Factor: 2.59 · DOI: 10.1021/ie2007467

4 AUTHORS, INCLUDING:

W. or W.X. Que
Xi'an Jiaotong University
220 PUBLICATIONS **2,185** CITATIONS
SEE PROFILE

Yulong Liao
University of Electronic Science and Technol…
46 PUBLICATIONS **347** CITATIONS
SEE PROFILE

Xingtian Yin
Xi'an Jiaotong University
36 PUBLICATIONS **381** CITATIONS
SEE PROFILE

I&EC research
Industrial & Engineering Chemistry Research

ARTICLE

pubs.acs.org/IECR

Photocatalytic Activity of TiO_2 Nanoparticles Sensitized by $CuInS_2$ Quantum Dots

Fengyu Shen, Wenxiu Que,* Yulong Liao, and Xingtian Yin

Electronic Materials Research Laboratory, School of Electronic and Information Engineering, Xi'an Jiaotong University, Xi'an 710049, Shaanxi, People's Republic of China

Supporting Information

ABSTRACT: In this paper, *p*-type $CuInS_2$ quantum dots are synthesized by a solvothermal route and incorporated with *n*-type TiO_2 nanoparticles by a thermal treatment process. Transmission electron microscopy (TEM) results indicate that the $CuInS_2$ quantum dots distribute uniformly and the size is ~3.4 nm. Photocatalytic activities of the TiO_2 nanoparticles sensitized with the $CuInS_2$ quantum dots are evaluated by the degradation of the methyl orange aqueous solution under ultraviolet (UV) and visible (vis) light irradiation and show an enhanced performance, compared with the pure TiO_2 nanoparticles and the pure $CuInS_2$ quantum dots. Microstructural, morphological, and optical properties of the TiO_2 nanoparticles sensitized with the $CuInS_2$ quantum dots are characterized by X-ray diffraction (XRD) analysis, TEM, and UV−vis absorption spectroscopy. Results indicate that the $CuInS_2$ quantum dots greatly enhance the absorption of UV and visible light due to the *p*−*n* heterojunction being constructed between *p*-type $CuInS_2$ quantum dots, and *n*-type TiO_2 nanoparticles. Effects of the mass ratio of the TiO_2 and $CuInS_2$ and the thermal treatment temperature on the photocatalytic activities of the TiO_2 nanoparticles sensitized with the $CuInS_2$ quantum dots are also investigated.

1. INTRODUCTION

TiO_2, as an oxide semiconductor, has been used in many aspects, such as photovoltaics, photocatalysis, sensors, and biomedical science, because of its high chemical stability, nontoxicity, easy availability, and higher redox potential of generated electron−hole pairs.[1−4] Therefore, different types of nanostructures of TiO_2, such as nanoparticles, nanotubes, nanospheres, nanorods, and nanowires, have been investigated, and great progress has been made in recent years.[5−9] TiO_2 doped with a cation or anion or both are becoming popular,[10,11] but doping has its own disadvantage, which probably causes defects within the band gap of the semiconductor to trap photogenerated charge carriers and decreases its activity.[12] Recently, coupling of semiconductors with other semiconductors, metals, and molecules to form a heterojunction structure has been widely used to enhance the photocatalytic performance of photocatalysts.[13,14]

Although TiO_2 is regarded as the most efficient and environmentally benign, its large band gap, along with a fast recombination rate of the photogenerated electron−hole pairs, hinders its photocatalytic activity and limits its further commercialization and industrial applications. There are many routes to overcome such an impediment, one of which is to introduce different semiconductors with narrow band gaps. For instance, the TiO_2/CdS heterojunction has been widely studied to decompose contamination effectively.[15−17] Here, the CdS, which has a narrow band gap, acts as a visible-light sensitizer and is also responsible for effective charge separation, to suppress the recombination process in the nanojunction. However, in view of recent environmental regulations, the intrinsic toxicity of the cadmium casts doubt on the future applicability of the cadmium compounds, despite their great optical and electrical properties. Thus, several Cd-free alternative materials, including I−III−VI_2 compounds, have been proposed to replace CdS.

$CuInS_2$, with a band gap of 1.5 eV, is a direct-band- gap semiconductor with a high optical absorption coefficient and is widely used in solar cells, because its band-gap energy is at the red edge of the solar spectrum.[18,19] Recently, several methods have been reported to synthesize high-quality and monodispersed $CuInS_2$ quantum dots in the nonaqueous phase.[20−22] However, to the best of our knowledge, there have been a few reports on photocatalytic activity of the TiO_2 nanoparticles sensitized by the $CuInS_2$ quantum dots. Kang[23] has reported the photocatalytic activities of the TiO_2 nanoparticles incorporated with $CuInS_2$ clusters. In his method, the $CuInS_2$ clusters were synthesized based on the TiO_2 nanoparticles. Recently, research about the photocatalytic activities of the deposition of $CuInS_2$ nanoparticles onto TiO_2 nanotube arrays has been also reported.[24] Here, we report a new study on the TiO_2/$CuInS_2$ (the TiO_2 nanoparticles sensitized by the $CuInS_2$ quantum dots) two-component nanojunction system. Both of the semiconductors are prepared separately and then were blended together at a low annealing temperature, to form a heterojunction structure. The photocatalytic activity of the TiO_2/$CuInS_2$ heterojunction is investigated by evaluating the photocatalytic degradation of the methyl orange aqueous solution at room temperature. Surprisingly, a high photocatalytic activity of the sample is shown and a reasonable explanation for such a high photocatalytic activity is also presented.

2. EXPERIMENTAL SECTION

2.1. Materials. 1-Dodecanethiol (DDT, 97%) and 1-octadecene (ODE, 90%) were purchased from Jingchun Reagent Co.,

Received: April 7, 2011
Accepted: June 26, 2011
Revised: June 18, 2011
Published: June 26, 2011

dx.doi.org/10.1021/ie2007467 | *Ind. Eng. Chem. Res.* 2011, 50, 9131–9137

Ltd. (China). Copper(I) chloride (CuCl), indium(III) chloride tetrahydrate ($InCl_3 \cdot 4H_2O$), sulfur powder (S), and all other products were purchased from Sinopharm Group Chemical Reagent Co., Ltd. (China). All the chemicals used in our experiment were received from commercial companies without any further purification, and they are analytical-grade reagents. Deionized water with a resistance of 18.3 MΩ cm was used in the experiment.

2.2. Preparation of $CuInS_2$ Quantum Dots. $CuInS_2$ quantum dots were synthesized by the solvothermal method reported in ref 25. Briefly, 0.019 g (0.2 mmol) of CuCl and 0.058 g(0.2 mmol) of $InCl_3 \cdot 4H_2O$ were mixed with 2 mL (8.25 mmol) of DDT and 8 mL of ODE in a three-neck flask under a nitrogen atmosphere. The mixture was heated to 80 °C under magnetic stirring for 30 min, then heated to the reaction temperature of 220 °C quickly and incubated for 30 min. Subsequently, the reaction vessel was allowed to cool to room temperature. Black $CuInS_2$ quantum dots were isolated by adding chloroform, precipitating with ethanol, and centrifuging at a speed of 10 000 rpm for 5 min. The sediment was then redispersed in chloroform. The precipitation/dispersion cycle was repeated twice in order to eliminate byproducts and unreacted precursors. Thus, black $CuInS_2$ powders were obtained by drying the black suspension in an oven at 80 °C.

2.3. Formation of TiO_2/$CuInS_2$ Heterojunction. Degussa P25 with an average particle size of ~25 nm was chosen as the TiO_2 nanoparticles to fabricate the heterojunction structure with the $CuInS_2$ quantum dots. The $CuInS_2$ quantum dots were first dispersed in chloroform and the TiO_2 nanoparticles were then injected. The two types of materials were mixed through stirring until the solvent was completely volatilized. Finally, the TiO_2/$CuInS_2$ heterojunction photocatalyst was obtained by annealing the mixture at different temperatures.

2.4. Characterization. X-ray diffraction (XRD) analysis was employed to characterize the crystallinity of the as-synthesized $CuInS_2$ quantum dots and the TiO_2 nanoparticles, which employs a D/max 2400 X Series X-ray diffractometer. The X-ray radiation source, obtained at 40 kV, 100 mA, was Cu Kα, and the scanning speed was 10° min^{-1} at a step of 0.02°. A transmission electron microscopy (TEM) system, consisting of a JEOL Model 2010F TEM microscope operating at 300 KeV, was used to observe the morphological properties of the samples. A field-emission scanning electron microscopy (FE-SEM) system that was equipped with a energy-dispersive X-ray detector (EDX) (Model JSM-6700F, JEOL, Inc., Japan) was used to characterize the composition of the samples. The UV−vis absorption spectra of the samples were obtained by a JASCO Model V-570 UV/vis/NIR spectrometer.

2.5. Photocatalytic Activity Measurement. The photocatalytic activities of the as-prepared TiO_2/$CuInS_2$ heterojunction photocatalysts were evaluated based on the degradation of the methyl orange aqueous solution, using a high-pressure mercury lamp (300 W) as a light source, which emits light in the UV range and the visible region. No filter was used. A methyl orange aqueous solution with a concentration of 20 mg/L was selected as the photocatalytic probe, and the concentration of the photocatalyst was 30 mg/100 mL in a methyl orange aqueous solution. The measurements were carried out in open air with magnetically stirring. Certain volume of the suspension solution was withdrawn at a sequence of time intervals. After disposal of the photocatalyst by a centrifugation, the residual methyl orange aqueous solution was measured by the UV−vis spectrophotometer at 463 nm, based on the Beer−Lambert Law:[26]

$$\text{Abs} = \varepsilon bc \tag{1}$$

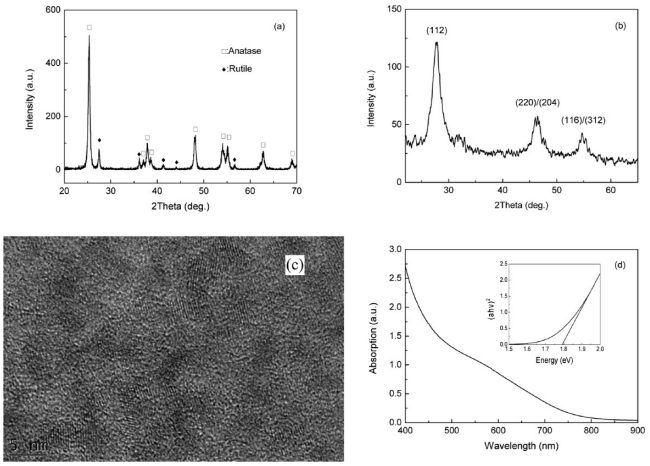

Figure 1. (a) XRD pattern of the TiO_2 nanoparticles; (b) XRD pattern of the $CuInS_2$ quantum dots; (c) typical TEM image of the $CuInS_2$ quantum dots; and (d) optical absorption spectrum of the $CuInS_2$ quantum dots. The inset shows the corresponding plots of $(\alpha h\nu)^2$ against photon energy ($h\nu$).

where Abs is the measured absorbance, ε the wavelength-dependent molar absorptive coefficient, and b the path length. The analyte concentration is given as $c/c_0 = A/A_0$; thus, the value of $c/c_0 = A/A_0$ can be easily obtained, where c_0 represents the initial concentration of the methyl orange aqueous solution, c the concentration after irradiation, A_0 the initial absorbance value of the methyl orange aqueous solution, and A the absorbance after irradiation. The degradation efficiency can be thus calculated according to the following equation:

$$\text{degradation}\ (\%) = \frac{A_0 - A}{A_0} \times 100 \tag{2}$$

3. RESULTS AND DISCUSSION

Figure 1a shows the XRD pattern of the TiO_2 nanoparticles. As one knows, P25 is composed of a mixed phase of the anatase and the rutile; thus, the characteristic peaks of both the anatase titania and the rutile titania are observed. Generally, TiO_2 with an anatase structure exhibits better photocatalytic activity,[27] but it has been also demonstrated that the anatase powders with an addition of a small fraction of rutile or brookite powders show an enhanced photocatalytic activity, because the electron and hole can transfer between the two phases.[28] Figure 1b shows the XRD pattern of the as-synthesized $CuInS_2$ quantum dots. The major diffraction peaks observed at 27.88°, 46.43°, and 54.99° can be indexed to the (112), (220)/(214), and (116)/(312) reflection direction of the chalcopyrite crystal structure of the $CuInS_2$ quantum dots, respectively. Using the Debye−Scherrer formula for the (112) direction, the size of the as-synthesis $CuInS_2$ quantum dots can be calculated: the value is ~3.8 nm. Figure 1c shows the TEM image of the $CuInS_2$ quantum dots synthesized at 220 °C for 30 min and deposited on an amorphous carbon grid. It can be observed that the as-synthesized $CuInS_2$ quantum dots have a narrow size distribution. According to the size distribution histogram as shown in Figure S1 in the Supporting Information, nanoparticles with a mean diameter of ~3.4 nm, which is close to the size calculated from the XRD measurement, are clearly observed. Moreover, the composition of the $CuInS_2$ quantum dots is obtained by EDX analysis, as

shown in Figure S2 in the Supporting Information, and the result indicates that the atomic ratio of the Cu/In/S is 0.9:1.1:2. In addition, the absorption spectrum of the $CuInS_2$ quantum dots dispersed in chloroform is also presented in Figure 1d, which shows a broad shoulder band with a long tail at longer wavelength and a broad absorption peak near 550 nm. According to the Kubelka−Munk formula,[29] the band gap of the as-synthesized $CuInS_2$ quantum dots is shown in the inset of Figure 1d: its value is ∼1.8 eV.

Figure 2 shows the photocatalytic activities of the pure TiO_2 nanoparticles (Degussa P25) and the $TiO_2/CuInS_2$ heterojunction photocatalysts for the degradation of the methyl orange aqueous solution. In order to evaluate an effect of the content of the $CuInS_2$ quantum dots on the photocatalytic activity of the as-prepared heterojunction photocatalysts, the photocatalytic activities of the $TiO_2/CuInS_2$ heterojunction photocatalysts with various mass ratios of TiO_2 (the TiO_2 nanoparticles) and $CuInS_2$ (the $CuInS_2$ quantum dots) were investigated under UV and visible light irradiation. All the samples were annealed at 300 °C under a nitrogen atmosphere. It can be found from Figure.2 that the pure TiO_2 sample has a great photocatalytic activity, but the $TiO_2/CuInS_2$ samples exhibit an enhanced photocatalytic activity if the mass ratio is at an appropriate value. For example, when the mass ratio of TiO_2 and $CuInS_2$ is 5:1, the best photocatalytic activity can be achieved. With the content of the $CuInS_2$ quantum dots increases, the photocatalytic activity of the $TiO_2/CuInS_2$ samples increases first and then weakens gradually. These results indicate that the content of the $CuInS_2$ quantum dots plays an important role for the photocatalytic degradation of the methyl orange aqueous solution. In order to better understand the photocatalytic activity of the heterojunction structure photocatalysts, a type of cationic dye (such as rhodamine (10 mg/L)) was also selected as the indicator, for comparison. The results are shown in Figure S3 in the Supporting Information, from which it can be observed that the photocatalytic activity of the $TiO_2/CuInS_2$ sample with a mass ratio of 5:1 is slightly higher than that of the pure TiO_2 sample.

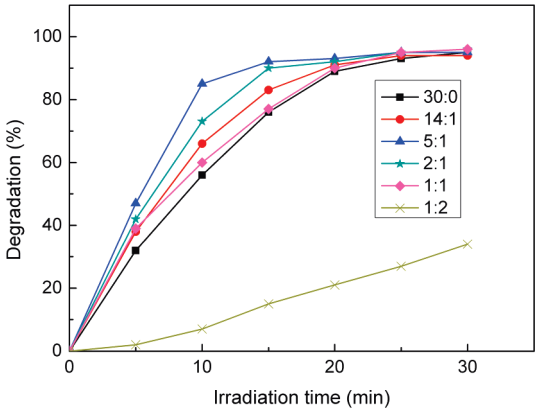

Figure 2. Photocatalytic degradation of the methyl orange aqueous solution catalyzed by the $TiO_2/CuInS_2$ photocatalysts with different mass ratios of TiO_2 and $CuInS_2$.

To visualize the hybridization between the TiO_2 nanoparticles and the $CuInS_2$ quantum dots in the $TiO_2/CuInS_2$ samples, the samples with mass ratios of 14:1 and 5:1 were characterized by TEM. Figure 3 presents the representative TEM images of these samples. Figure 3a, which shows the sample with 6.7 wt % of the $CuInS_2$ quantum dots, shows that the $CuInS_2$ quantum dots are sporadic and adhered to the TiO_2 nanoparticles compactly. Figure 3b shows a high-resolution transmission electron microscopy (HRTEM) image of the same sample shown in Figure 3a. The visible lattice fringe indicates that the TiO_2 and the $CuInS_2$ coexist. It can be seen from Figure 3c, which involves the sample with 16.7 wt % of the $CuInS_2$ quantum dots, that the heterojunctions between the TiO_2 nanoparticles and the $CuInS_2$ quantum dots are constructed. Interestingly, it can be clearly

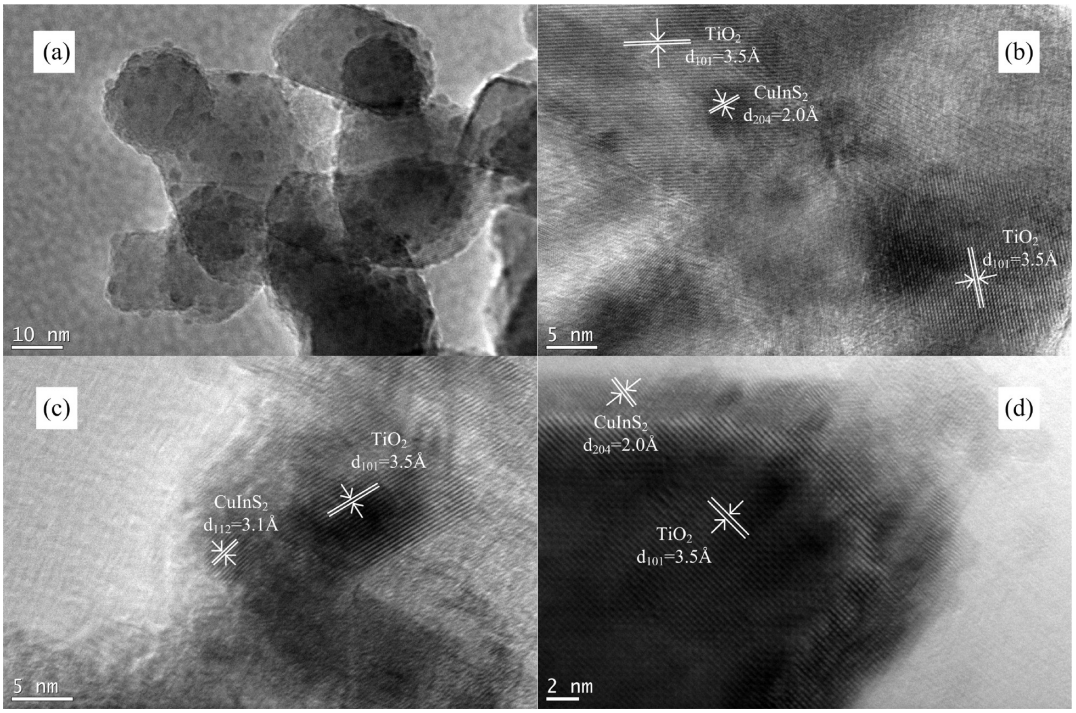

Figure 3. Typical TEM images of the $TiO_2/CuInS_2$ samples with different mass ratios: (a, c) 14:1 and (b,d) 1:2.

dx.doi.org/10.1021/ie2007467 |*Ind. Eng. Chem. Res.* 2011, 50, 9131–9137

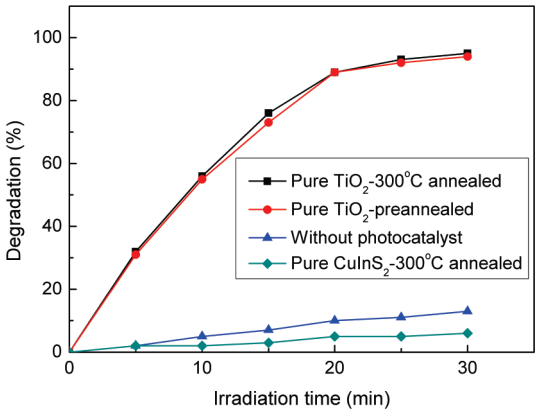

Figure 4. Photocatalytic degradation of the methyl orange aqueous solution catalyzed by different photocatalysts.

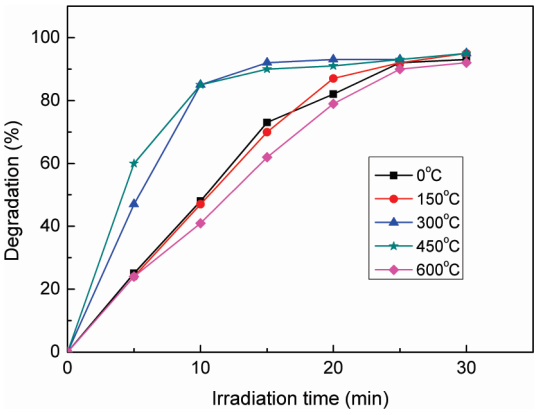

Figure 5. Photocatalytic degradation of the methyl orange aqueous solution catalyzed by the $TiO_2/CuInS_2$ sample with a mass ratio of 5:1 at different thermal treatment temperatures.

observed from Figure 3d that the TiO_2 nanoparticles are surrounded by a layer of the $CuInS_2$ quantum dots. The heterojunction structure shown in Figure 3d greatly improves the photocatalytic activities of the sample. In addition, the content of the $CuInS_2$ quantum dots affects the dispersal of the photocatalysts. Considering that the dispersal of P25 is better than that of the $CuInS_2$ quantum dots in aqueous solution, it is therefore impossible that the $TiO_2/CuInS_2$ photocatalyst is effectively dispersed in the solution if the mass of the $CuInS_2$ quantum dots is too great. The EDX analysis of the two samples is shown in Table S1 in the Supporting Information, which indicates that, after a heat treatment, the content of the $CuInS_2$ quantum dots in the two photocatalysts decreases from 6.7% and 16.7% to 4.4% and 11.0%, respectively. It should be ascribed to the decomposition of the organics capping the $CuInS_2$ quantum dots, and the loss of some indium and sulfur, which occurs during the heat-treatment process.

We also investigated the photocatalytic activities of the pure $CuInS_2$ quantum dots and the pure TiO_2 nanoparticles annealed at 300 °C, as shown in Figure 4. It can be seen from the blank test that only 13% of the methyl orange is photodegraded in 30 min, indicating that the methyl orange is stable enough to be the probe for the investigation of the photocatalytic properties of the as-prepared photocatalysts. It can be also seen from Figure 4 that the anneal process (under 300 °C) does not obviously affect the photocatalytic activity of the pure TiO_2 nanoparticles (P25), and the pure $CuInS_2$ quantum dots not only have no photocatalytic activity, but also inhibit the photolysis of the methyl orange. It is probably related to the fact that the pure $CuInS_2$ quantum dots disperse poorly in aqueous solution, and they absorb most UV and visible light through the aqueous solution, but the photogererated electron−hole pairs cannot be separated effectively.

In order to further explore the photocatalytic activity of the sample with the mass ratio of 5:1 (TiO_2:$CuInS_2$), the samples were studied by changing the heat-treatment temperature. Figure 5 shows the photocatalytic activities of the samples annealed at 0, 150, 300, 450, and 600 °C under a nitrogen atmosphere. As shown in Figure 5, the samples annealed at 300 or 450 °C have the highest photocatalytic activities. It is also easy to see that, with increasing thermal treatment temperature, the photocatalytic activity of the $TiO_2/CuInS_2$ photocatalyst first is enhanced and then weakens. When the thermal treatment temperature is <150 °C, the combination between TiO_2 and $CuInS_2$ is probably not so compact that the electrons and holes cannot transfer each other between them; that is to say, the $p-n$ heterojunction between p-$CuInS_2$ and n-TiO_2 is not constructed at such a low temperature. However, when the thermal treatment temperature is increased up to 600 °C, the size of the $CuInS_2$ particles is also enlarged to over 20 nm (according to the Debye−Scherrer formula), showing a size comparable to that for the TiO_2 nanoparticles. Thus, the large size of the $CuInS_2$ particles leads to the disappearance of the quantum confinement effect. A recycling test of the photocatalytic activity of the sample annealed at 300 °C was carried out, and the results are shown in Figure S4a in the Supporting Information. The corresponding mean photocatalytic activity with error bars is shown in Figure S4b in the Supporting Information, indicating that the standard error is small. That is to say, the photocatalytic activity changes little from the first time to the fourth time. Figure 6 shows the XRD patterns of the TiO_2 nanoparticles and of the $CuInS_2$ quantum dots annealed at different temperatures. Figure 6a is the XRD patterns of the TiO_2 nanoparticles annealed from 0 °C to 600 °C. It can be seen that the crystalline property of the TiO_2 nanoparticles is almost unchanged and there is no any phase transition to be detected. Figure 6b shows the crystalline property of the $CuInS_2$ quantum dots measured on silicon substrate and annealed at different temperatures, indicating that the crystalline property of the $CuInS_2$ quantum dots is obviously enhanced as the thermal treatment temperature increases. Especially, when the thermal treatment temperature increases up to 600 °C, the peak at 32.30° indexed to the (200) reflection direction of the chalcopyrite crystal structure can be clearly observed, but the size of the $CuInS_2$ quantum dots is also obviously enlarged as the thermal treatment temperature is increased. Moreover, the XRD results of some $TiO_2/CuInS_2$ samples with different mass ratios and different heat treatment temperatures are investigated, which are shown in Figure S5 in the Supporting Information. It is difficult to detect the peaks of $CuInS_2$, because of its low content.

The photocatalytic degradation of the methyl orange aqueous solution can be regarded as a pseudo-first-order reaction. Therefore, its kinetics can be expressed by the following formula:[30]

$$C_t = C_0 e^{-kt} \quad (3)$$

where k (min^{-1}) is the degradation rate constant, C_t the methyl orange concentration at reaction time t, and C_0 the initial methyl

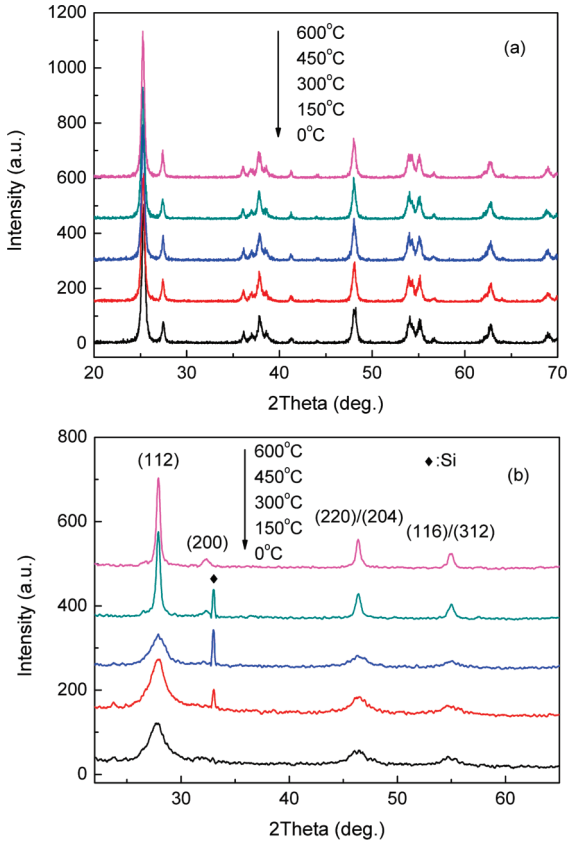

Figure 6. XRD patterns of (a) the TiO_2 nanoparticles and (b) the $CuInS_2$ quantum dots annealed at different temperatures.

Table 1. Degradation Rate Constant (k) Values for Different Photocatalysts

photocatalyst	k (min^{-1})
null	0.005
pure $CuInS_2$-300 °C	0.003
pure TiO_2	0.080
pure TiO_2-300 °C	0.085
TiO_2/$CuInS_2$-14:1-300 °C	0.107
TiO_2/$CuInS_2$-5:1-300 °C	0.162
TiO_2/$CuInS_2$-2:1-300 °C	0.131
TiO_2/$CuInS_2$-1:1-300 °C	0.096
TiO_2/$CuInS_2$-1:2-300 °C	0.008
TiO_2/$CuInS_2$-5:1	0.070
TiO_2/$CuInS_2$-5:1-150 °C	0.066
TiO_2/$CuInS_2$-5:1-450 °C	0.165
TiO_2/$CuInS_2$-5:1-600 °C	0.057

orange concentration. According to eq 3, the degradation rate constant of the samples can be calculated and their values are listed in Table 1. It can be seen from Table 1 that the value of the degradation rate constant (k) of the TiO_2/$CuInS_2$ photocatalyst with the mass ratio of 5:1 (TiO_2:$CuInS_2$) and annealed at 450 °C is up to 0.165 min^{-1}, which is as twice as that of the pure TiO_2 nanoparticles without any thermal treatment (0.080 min^{-1}). It should be stressed here that all the results presented in Table 1 are consistent with those revealed in Figures 2, 4, and 5.

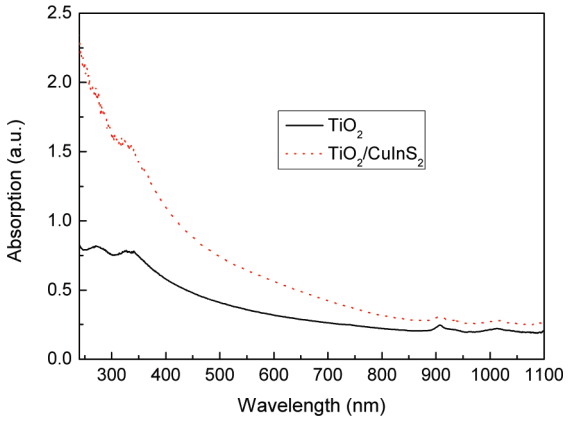

Figure 7. Optical absorption spectra of the TiO_2 nanoparticles and the TiO_2/$CuInS_2$ sample with the mass ratio of 5:1 (TiO_2:$CuInS_2$). Both samples are annealed at 300 °C for 15 min.

Figure 7 shows the absorption spectra of the pure TiO_2 nanoparticles and the TiO_2/$CuInS_2$ sample annealed at 300 °C. The mass ratio of the TiO_2 nanoparticles and the $CuInS_2$ quantum dots in the TiO_2/$CuInS_2$ sample is 5:1. It can be seen that the pure TiO_2 nanoparticles have a strong absorption in the UV light region. Compared to the pure TiO_2 nanoparticles, the absorbance of the TiO_2/$CuInS_2$ sample has an obvious increase in UV and visible light regions, which should be ascribed to the absorption of the $CuInS_2$ quantum dots, as shown in Figure 1d. That is to say, the TiO_2/$CuInS_2$ sample has a more intense absorption for the UV and visible light, which is probably responsible for the enhanced photocatalytic activity, compared to the pure TiO_2 nanoparticles. In addition, the $p-n$ heterojunction between TiO_2 and $CuInS_2$ also has a contribution to the enhanced photocatalytic activity. It is well-known that TiO_2 is an n-type semiconductor and $CuInS_2$ is a p-type semiconductor. Thus, when p-$CuInS_2$ and n-TiO_2 are blended together, followed by a thermal treatment, the $p-n$ heterojunctions can be formed in the two types of semiconductors and the build-in electric field is thus formed from n-TiO_2 to p-$CuInS_2$. Therefore, the photogenerated electron−hole pairs due to UV and visible light illumination can be effectively separated with electrons flowing into n-type TiO_2 and holes flowing into p-type $CuInS_2$.

In order to further explore other possible reasons for the enhanced photocatalytic activities of the TiO_2/$CuInS_2$ photocatalysts, the separation process of the photoexcited electron−hole pairs is also investigated as shown in Figure 8. It has been well-reported that the band gap of TiO_2 is ~3.2 eV, which can be only excited by photons with wavelengths of <388 nm, while $CuInS_2$ in our experiment can be only excited by photons with wavelengths of <690 nm (1.8 eV). When the energy of the incident light is <1.8 eV, no electron−hole pairs will be excited, which is shown in Figure 8a. For the case of incidence light whose energy is in the range of 1.8−3.2 eV, a photon excites an electron from the valence band of $CuInS_2$ to the conduction band and the electron is then transferred to the conduction band of TiO_2, as shown in Figure 8b. For the case of incidence light whose energy is in the range of 3.2−3.6 eV, a photon generates one electron−hole pair of the $CuInS_2$ quantum dots and the electron−hole pairs of the TiO_2 nanoparticles can be generated. At the same time, the holes excited in the valence band of TiO_2 are transferred to the valence band of $CuInS_2$, while the electrons are transferred to the opposite direction on the conduction band,[31] which is the situation that

dx.doi.org/10.1021/ie2007467 |Ind. Eng. Chem. Res. 2011, 50, 9131–9137

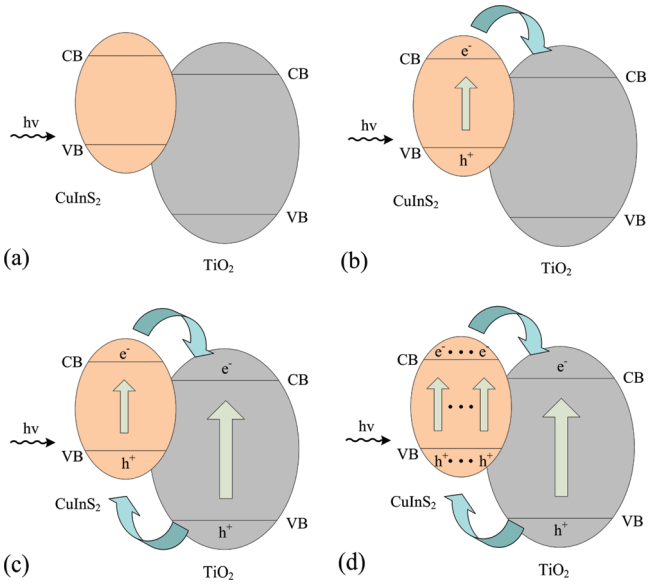

Figure 8. Schematic diagram of the photogenerated electron−hole separation process with the cases of incidence light whose energy is in the range of (a) ≤1.8 eV, (b) 1.8−3.2 eV, (c) 3.2−3.6 eV, and (d) ≥3.6 eV.

is shown in Figure 8c. For the case of incidence light whose energy is >3.6 eV, a photon can generate multiple electron−hole pairs for $CuInS_2$ quantum dots because of the quantum confinement effect,[32] which is also displayed in Figure 8d. However, in our experiment, only the latter three types of situations can happen, because our light source is a high-pressure mercury lamp (300 W) that only emits UV and visible light.

4. CONCLUSIONS

successful synthesis and integration of *p*-type $CuInS_2$ quantum dots with *n*-type TiO_2 nanoparticles to form *p*−*n* heterojunctions through the thermal treatment process has been achieved. The photocatalytic activities of the TiO_2/$CuInS_2$ heterojunction photocatalysts composed with different mass ratios of TiO_2 and $CuInS_2$ have been investigated under ultraviolet (UV) and visible (vis) light illumination. The optimal mass ratio of TiO_2 to $CuInS_2$ has been obtained, and the value is 5:1. Effects of the thermal treatment temperature on the photocatalytic activity also have been investigated; the optimum temperature is from 300 °C to 450 °C, and the highest degradation rate for the methyl orange aqueous solution has been calculated, which is more than 0.16/min. An interesting phenomenon is noted that the naked $CuInS_2$ quantum dots have the ability to restrain the photolysis of the methyl orange. The enhanced photocatalytic activities of the TiO_2/$CuInS_2$ heterojunction photocatalysts are ascribed to the enhanced absorption of UV and vis light by the $CuInS_2$ quantum dots, and the photogenerated electron−hole pairs can be effectively separated by the *p*−*n* heterojunction constructed by *n*-type TiO_2 and *p*-type $CuInS_2$.

■ ASSOCIATED CONTENT

Supporting Information. Size distribution histogram, EDX analysis, photodegradation of rhodamine, recycling test, and raw data of Figures 2, 4, and 5. The information is available free of charge via the Internet at http://pubs.acs.org/.

■ AUTHOR INFORMATION

Corresponding Author

*Tel.: +86-29-82668679. Fax: +86-29-82668794. E-mail address: wxque@mail.xjtu.edu.cn.

■ ACKNOWLEDGMENT

This work was supported by the Major Program of the National Natural Science Foundation of China (under Grant No. 90923012), the Ministry of Science and Technology of China through 863-project (under Grant No. 2009AA03Z218), and the Research Fund for the Doctoral Program of Higher Education of China (under Grant No. 200806980023).

■ REFERENCES

(1) Li, T. L.; Teng, H. S. Solution synthesis of high-quality $CuInS_2$ quantum dots as sensitizers for TiO_2 photoelectrodes. *J. Mater. Chem.* **2010**, *20*, 3656–3664.

(2) O'Rourke, C.; Mills, A. Adsorption and photocatalytic bleaching of acid orange 7 on P25 titania. *J. Photochem. Photobiol. A: Chem.* **2010**, *216*, 261–267.

(3) Zheng, S.; Cai, Y.; O'Shea, K. E. TiO_2 photocatalytic degradation of phenylarsonic acid. *J. Photochem. Photobiol. A: Chem.* **2010**, *210*, 61–68.

(4) Karunakaran, C.; Abiramasundari, G.; Gomathisankar, P.; Manikandan, G.; Anandi, V. Cu-doped TiO_2 nanoparticles for photocatalytic disinfection of bacteria under visible light. *J. Colloid Interface Sci.* **2010**, *352*, 68–74.

(5) Choi, H.; Stathatos, E.; Dionysiou, D. D. Effect of surfactant in a modified sol on the physicochemical properties and photocatalytic activity of crystalline TiO_2 nanopartices. *Top. Catal.* **2007**, *44*, 513–521.

(6) Foong, T. R. B.; Shen, Y. D.; Hu, X.; Sellinger, A. Template-directed liquid ALD growth of TiO_2 nanotube arrays: properties and potential in photovoltaic devices. *Adv. Funct. Mater.* **2010**, *20*, 1390–1396.

(7) Bullen, H. A.; Garrett, S. J. TiO_2 nanoparticle arrays prepared using a nanosphere lithography technique. *Nano Lett.* **2002**, *2*, 749–745.

(8) Zhu, H. M.; Yang, B. F.; Xu, J.; Fu, Z. P.; Wen, M. W.; Guo, T.; Fu, S. Q.; Zuo, J.; Zhang, S. Y. Construction of Z-scheme type CdS−Au−TiO_2 hollow nanorod arrays with enhanced photocatalytic activity. *Appl. Catal., B* **2009**, *90*, 463–469.

(9) Nisar, J.; Araujo, C. M.; Ahuja, R. Water interaction with native defects on rutile TiO_2 nanowire: Ab initio calculations. *Appl. Phys. Lett.* **2011**, *98*, 083115.

(10) Kumaresan, L.; Mahalakshmi, M.; Palanichamy, M.; Murugesan, V. Synthesis, characterization, and photocatalytic activity of Sr^{2+} doped TiO_2 nanoplates. *Ind. Eng. Chem. Res.* **2010**, *49*, 1480–1485.

(11) Cheng, Y. H.; Huang, Y. Z.; Kanhere, P. D.; Subramaniam, V. P.; Gong, D. G.; Zhong, S.; Highfield, J.; Schreyer, M. K.; Chen, Z. Dual-phase titanate/anatase with nitrogen doping for enhanced degradation of organic dye under visible light. *Chem.—Eur. J.* **2011**, *17*, 2572–2578.

(12) Sasikala, R.; Shirole, A. R.; Sudarsan, V.; Kamble, V. S.; Sudakar, C.; Naik, R.; Rao, R.; Bharadwaj, S. R. Role of support on the photocatalytic activity of titanium oxide. *Appl. Catal., A* **2010**, *390*, 245–252.

(13) Chen, Y. S.; Crittenden, J. C.; Hackney, S.; Sutter, L.; Hand, D. W. Preparation of a novel TiO_2-based *p*−*n* junction nanotube photocatalyst. *Environ. Sci. Technol.* **2005**, *39*, 1201–1208.

(14) Kim, Y. J.; Gao, B.; Han, S. Y.; Jung, M. H.; Chakraborty, A. K.; Ko, T.; Lee, C.; Lee, W. I. Heterojunction of $FeTiO_3$ nanodisc and TiO_2 nanoparticle for a novel visible light photocatalyst. *J. Phys. Chem. C* **2009**, *113*, 19179–19184.

(15) Xie, Y.; Ali, G.; Yoo, S. H.; Cho, S. O. Sonication-assisted synthesis of CdS quantum-dot-sensitized TiO_2 nanotube arrays with

enhanced photoelectrochemical and photocatalytic activity. *ACS Appl. Mater. Interfaces* **2010**, *10*, 2910–2914.

(16) Chen, C.; Cai, W. M.; Long, M.; Zhou, B. X.; Wu, Y. H.; Wu, D. Y.; Feng, Y. J. Synthesis of visible-light responsive grapheme oxide/TiO_2 composites with *p*/*n* heterojunction. *ACS Nano* **2010**, *4*, 6425–6432.

(17) Zhao, W. X.; Bai, Z. P.; Ren, A. L.; Guo, B.; Wu, C. Sunlight photocatalytic activity of CdS modified TiO_2 loaded on activated carbon fibers. *Appl. Surf. Sci.* **2010**, *256*, 3493–3498.

(18) Scheer, R.; Walter, T.; Schock, H. W.; Fearheiley, M. L.; Lewerenz, H. J. $CuInS_2$ based thin film solar cell with 10.2% efficiency. *Appl. Phys. Lett.* **1993**, *63*, 3294–3296.

(19) Yue, W. J.; Han, S. K.; Peng., R. X.; Shen, W.; Geng, H. W.; Wu, F.; Tao, S. W.; Wang, M. T. $CuInS_2$ quantum dots synthesized by a solvothermal route and their application as effective electron acceptors for hybrid solar cells. *J. Mater. Chem.* **2010**, *20*, 7570–7578.

(20) Czekelius, C.; Hilgendorff, M.; Spanhel, L.; Bedja, I.; Lerch, M.; Muller, G.; Bloeck, U.; Su, D. S.; Giersig, M. A simple colloidal route to nanocrystalline ZnO/$CuInS_2$ bilayers. *Adv. Mater.* **1999**, *11*, 643–646.

(21) Zhong, H. Z.; Zhou, Y.; Ye, M. F.; He, Y. J.; Ye, J. P.; He, C.; Yang, C. H.; Li, Y. F. Controlled synthesis and optical properties of colloidal ternary chalcogenide $CuInS_2$ nanocrystals. *Chem. Mater.* **2008**, *20*, 6434–6443.

(22) Panthani, M. G.; Akhavan, V.; Goodfellow, B.; Schmidtke, J. P.; Dunn, L.; Dodabalapur, A.; Barbara, P. F.; Korgel, B. A. Synthesis if $CuInS_2$, $CuInSe_2$, and $Cu(In_xGa^{1-x})Se_2$ (CIGS) nanocrystal "ink" for printable photovoltaics. *J. Am. Chem. Soc.* **2008**, *130*, 16770–16777.

(23) Kang, S.; Yang, Y.; Bu, W.; Mu., J. TiO_2 nanoparticles incorporated with $CuInS_2$ clusters: Preparation and photocaralytic activity for degradation of 4-nitrophenol. *J. Solid State Chem.* **2009**, *182*, 2972–2976.

(24) Liu, R.; Liu, Y.; Liu, C.; Luo, S.; Teng, Y.; Yang, L.; Yang, R.; Cai, Q. Enhanced photoelectrocatalytic degradation of 2,4-dichlorophenoxyacetic acid by $CuInS_2$ nanoparticles deposition onto TiO_2 nanotube arrays. *J. Alloys Compd.* **2011**, *509*, 2434–2440.

(25) Li, L.; Daou, T. J.; Texier, I.; Tran, T. K. C.; Nguyen, Q. L.; Reiss, P. Highly luminescent $CuInS_2$/ZnS core/shell nanocrystals: Cadmium-free quantum dots for in vivo imaging. *Chem. Mater.* **2009**, *21*, 2422–2429.

(26) Ingle, J. D., Jr.; Crouch, S. R. *Spectrochemical Analysis*; Prentice Hall: Englewood Cliffs, NJ, 1988.

(27) Addamo, M.; Augugliaro, V.; Paola, A. D.; García-López, E.; Loddo, V.; Marcì, G.; Molinari, R.; Palmisano, L.; Schiavello, M. Preparation, characterization, and photoactivity of polycrystalline nanostructured TiO_2 catalysts. *J. Phys. Chem. B* **2004**, *108*, 3303–3310.

(28) Ohtani, B.; Prieto-Mahaney, O. O.; Li, D.; Abe, R. What is Degussa (Evonik) P25? Crystalline composition analysis, reconstruction from isolated pure particles and photocatalytic activity test. *J. Photochem. Photobiol. A: Chem.* **2010**, *216*, 179–182.

(29) Pankove, J. I. *Optical Processes in Semiconductors*; Dover: New York, 1971.

(30) Abdullah, A. Z.; Ling, P. Y. Heat treatment effects on the characteristics and sonocatalytic performance of TiO_2 in the degradation of organic dyes in aqueous solution. *J. Hazard. Mater.* **2010**, *173*, 159–167.

(31) Bessekhouad, Y.; Robert, D.; Weber, J. V. Photocatalytic activity of Cu_2O/TiO_2, Bi_2O_3/TiO_2 and $ZnMn_2O_4/TiO_2$ heterojunctions. *Catal. Today* **2005**, *101*, 315–321.

(32) Xu, G. Y.; Torres, C. M.; Song., E. B.; Tang, J. S.; Bai, J. W.; Duan, X. F.; Zhang, Y. G.; Wang, K. L. Enhanced conductance fluctuation by quantum confinement effect in grapheme nanoribbons. *Nano Lett.* **2010**, *10*, 4590–4594.